

Localized induction heating solder bonding for wafer level MEMS packaging

Hsueh-An Yang, Mingching Wu and Weileun Fang

Department of Power Mechanical Engineering, National Tsing Hua University, Hsinchu, Taiwan

E-mail: fang@pme.nthu.edu.tw

Received 29 July 2004

Published 8 December 2004

Online at stacks.iop.org/JMM/15/394

Abstract

This paper reports a new solder bonding method for the wafer level packaging of MEMS devices. Electroplated magnetic film was heated using induction heating causing the solder to reflow. The experiment results show that it took less than 1 min to complete the bonding process. In addition, the MEMS devices experienced a temperature of only 110 °C during bonding, thus thin film materials would not be damaged. Moreover, the bond strength between silicon and silicon wafer was higher than 18 MPa. The step height of the feed-through wire (acting as the electrical feed-through of the bonded region) is sealed by the electroplated film. Thus, the flatness and roughness of the electroplated surface are recovered by the solder reflow, and the package for preventing water leakage can be achieved. The integration of the surface micromachined devices with the proposed packaging techniques was demonstrated.

1. Introduction

Movable and deformable structures are frequently involved in MEMS devices such as accelerometers, pressure sensors, optical scanners, RF switches, etc. In general, these MEMS devices need to interact with the environment. Moreover, the yield of the suspended micromachined structures after experiencing the harsh environment of wafer dicing is another consideration. Therefore, the concept and purpose for the MEMS package cannot directly inherit from those of the traditional IC package. Wafer bonding techniques, such as anodic bonding and fusion bonding, are regarded as promising approaches for MEMS packaging. However, most of the existing bonding techniques are conducted at high temperature, 1000 °C, for the conventional fusion bonding temperature, and at 300–500 °C [1, 2] for anodic bonding. These high-temperature processes may induce thermal effect problems, and damage the micro structures or the integrated circuits. In [3, 4], a localized heating approach by an embedded heater was presented to prevent thermal problems during bonding.

In addition to thermal considerations, it is difficult to achieve a vacuum seal for a nonplanarized MEMS surface. For instance, the typical case is the MEMS device that has electrical interconnections with bond pads outside the vacuum-sealed cavity [5]. In this regard, a special wafer bonding

technique for the MEMS package is required [6]. The reflow of organic photoresist has been employed to solve the nonplanarized surface problem; however, an out-gassing effect has occurred [7, 8]. Glass frit bonding is another approach to overcome the nonplanarized surface; however, the feature size of the structure is limited by the screen printing process [9]. Solder reflow bonding is another solution for hermetic sealing, although the devices could be damaged by the global heating process.

This paper reports on the induction heating solder bonding approach for the integration of fabrication processes and wafer level packaging of MEMS devices. Although this heating approach has been very popular for bulk materials [10], the induction heating efficiency for micro-scale thin film is a primary concern. To demonstrate the feasibility of this approach, electroplated Ni/Co magnetic film and low melting point Pb/Sn solder were employed to realize a localized induction heating process, preventing a thermal problem due to bonding temperature. Additionally, the Sn/Pb solder reflow technique solves the nonplanarized surface problem, achieving an anti-leakage seal of the packaged device.

2. Concept and fabrication processes

Induction heating is a well-known technology for producing a temperature rise in some materials very quickly [11]. This

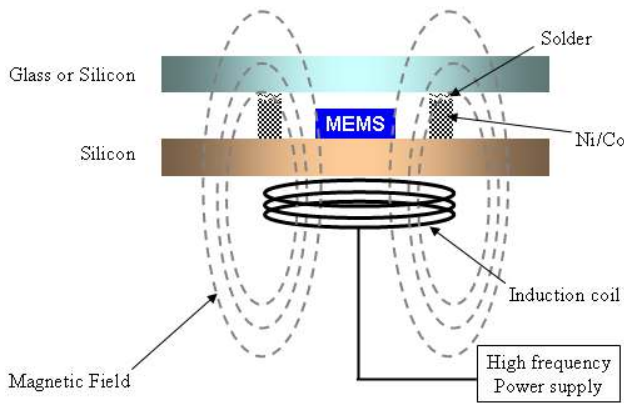


Figure 1. The schematic illustration for induction heating. The sample was placed inside a magnetic field provided by the coil underneath.

technology has been extensively employed to heat electrically conductive materials in applications such as melting, soldering and hardening of metals. As shown in figure 1, the induction heating system consists of a high-frequency power supply, an induction coil and the work pieces. An ac power supply drives the induction coil, generating a magnetic field. Meanwhile, an eddy current is developed in the work piece as it is placed inside the magnetic field. This causes heat to be generated by the work piece due to the eddy current loss and hysteresis loss [12]. According to the characteristics of the heating mechanism, the work piece can be noncontact and locally heated in some particular regions. For instance, the composite work piece in figure 1 consists of silicon, glass and metal parts. Using induction heating technology, a higher temperature will be generated at the metal parts, especially in the ferromagnetic Ni/Co alloy. These ferromagnetic materials can be exploited as a localized heating element for the composite work piece. Wafer level packaging can be realized if the whole wafer can be placed inside the magnetic field in figure 1.

This study has established the fabrication process required to conduct the presented bonding technique for silicon substrates. In addition, fabrication processes used to encapsulate the MUMPs devices by Si and glass covers by the presented bonding method have also been accomplished.

2.1. Si-Si bonding processes

A 4-inch single-side polished silicon wafer was deposited with 200 Å Cr as the adhesive layer and 200 Å Cu as the seed layer, as shown in figure 2(a). A Ni/Co alloy was electroplated on top of the seed layer to act as the spacer. The solutions for the electroplating of the Ni/Co are listed in table 1; in addition, the deposition rate was 0.1–0.2 $\mu\text{m min}^{-1}$ and the current density was 1–5 ASD (ampere/dm²). Since the Ni/Co alloy is a ferromagnetic material, it has a very large permeability [11]. Thus, a much higher temperature was generated by the Ni/Co spacer for a given driving current during the induction heating. The Sn/Pb alloy solder was electroplated on top of the spacer, as shown in figure 2(b). The electroplating solutions of the solder are listed in table 1; the deposition rate and the current density were 0.1–0.5 $\mu\text{m min}^{-1}$ and 1–4 ASD, respectively. The composition of the Sn/Pb solder was Sn–Pb (63/37), and its melting point was 183 °C.

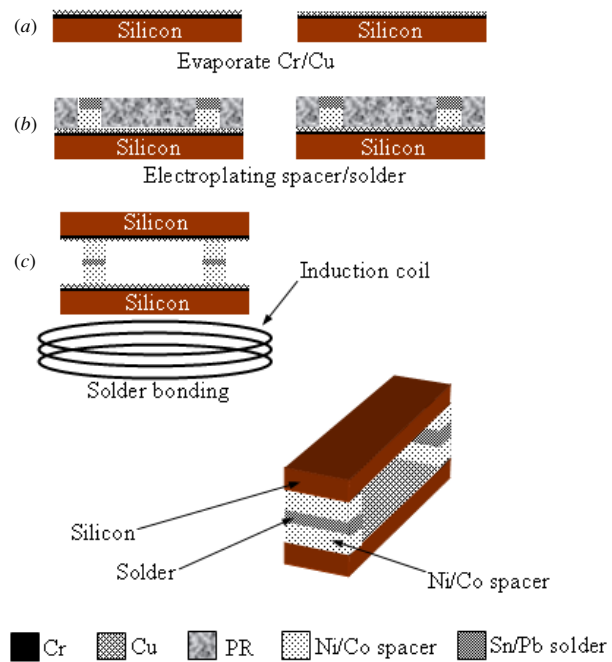


Figure 2. The concept and fabrication process for the present study.

Table 1. The plating solution for the electroplating of (a) Ni/Co and (b) Pb/Sn solder.

(a) Electroplating of Ni/Co	
Nickel sulfamate $\text{Ni}(\text{NH}_2\text{SO}_4)_2 \cdot 4\text{H}_2\text{O}$	450–550 ml l ⁻¹
Cobalt sulfamate $\text{Co}(\text{NH}_2\text{SO}_4)_2$	15–25 ml l ⁻¹
Nickel chloride $\text{NiCl}_2 \cdot 6\text{H}_2\text{O}$	2–7 g l ⁻¹
Boric acid H_3BO_3	30–50 g l ⁻¹
Stress reducer	2–10 ml l ⁻¹
(b) Electroplating of Pb/Sn solder	
Tin	12–18 g l ⁻¹
Lead	1.5–2.5 g l ⁻¹
pH value	3.0–5.0
Specific weight	1.1–1.2

The spacer and solder provided more than 50 μm of space to allow for a large range of motion of the MEMS devices. As shown in figure 1, the induction coil, driven with high-frequency ac current, provided the wafers with a magnetic field. After the two silicon wafers were aligned, the magnetic field was employed to heat the thin film Ni/Co magnetic spacer, as illustrated in figure 2(c). In this study, the process was performed at atmospheric pressure (1 atm). The induction heating temperature is significantly influenced by the magnetic field, the material property (permeability) and the area of the magnetic layer [11]. Hence, a large area Ni/Co alloy and a higher driving frequency were required for micro-scale induction heating. The driving frequency and current of the magnetic coil were 100 kHz and 25 A, respectively. Moreover, the width of the electroplated Ni/Co bonding ring is about 600 μm . It took only 15 s for the magnetic spacer to reach 200 °C using induction heating, at which point the solder on top of the spacer began to reflow. Thus, the two silicon wafers were bonded together through the solder.

The SEM photograph in figure 3(a) shows the typical result of silicon substrates after bonding. The sample was purposely broken so that the space provided by the spacer

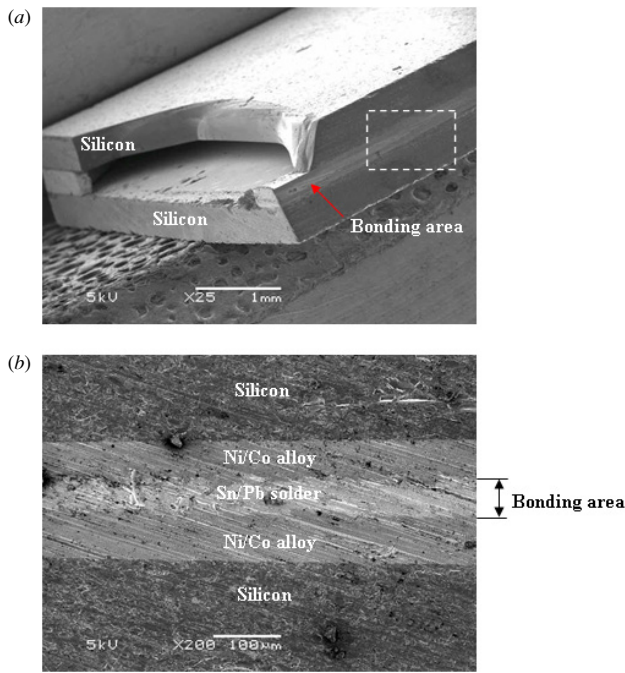


Figure 3. The SEM photographs of (a) the silicon substrates after bonding, and (b) the close-up of the bonded specimen in the dashed box region.

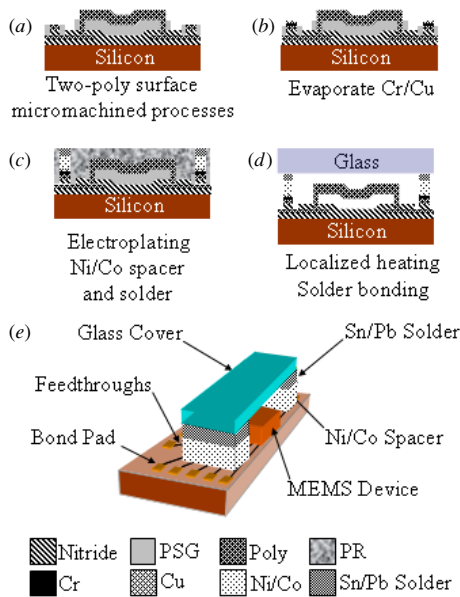


Figure 4. Fabrication process to integrate the surface micromachined devices with the present bonding method.

and solder could be clearly observed. The close-up SEM photograph in figure 3(b) shows a typical cross section of the bonded silicon–silicon test sample as indicated by the dashed box in figure 3(a). There are three different layers, including two Ni/Co spacer layers and one Sn/Pb solder layer, between the silicon substrates. According to the characteristics of solder reflow, no interface was observed in the bonded Sn/Pb layers.

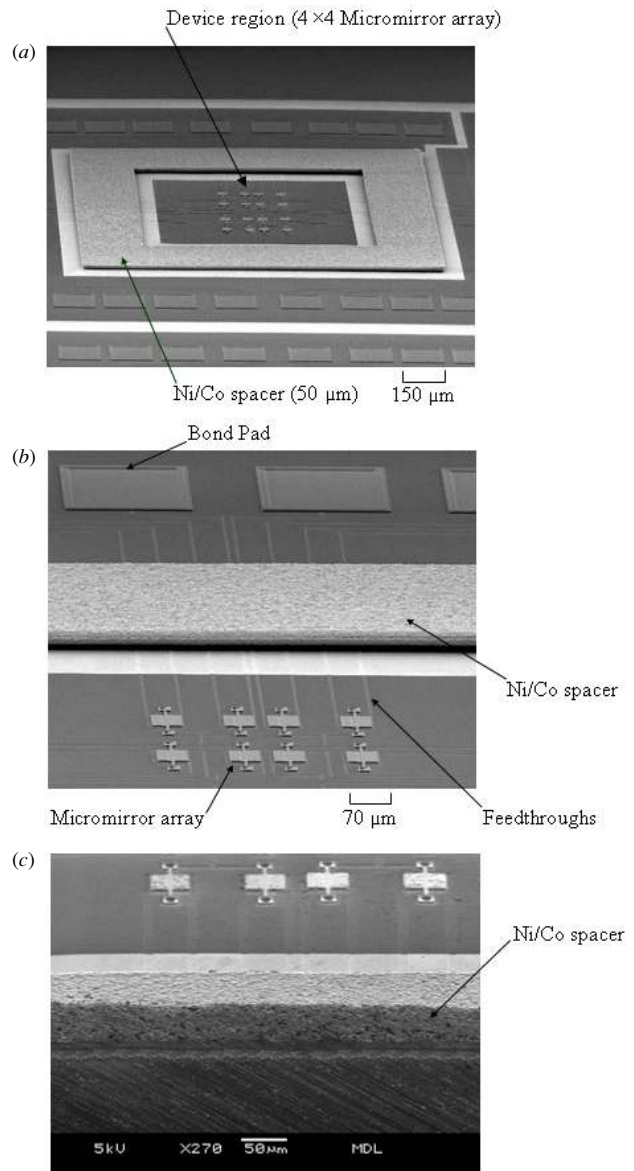


Figure 5. The SEM photographs of the integration of surface micromachined devices and the spacer (a) a 4×4 mirror array inside the $50 \mu\text{m}$ height Ni/Co spacer, (b) conducting wires and bonding pads of mirrors and (c) the microscopic section of the bonding region.

2.2. Integration of MUMPs and bonding processes

It is easy to integrate the presented localized bonding technique with other fabrication processes. Moreover, it is possible to employ this technique to bond silicon and glass. This study established a process, depicted in figure 4, to demonstrate the feasibility of integration of 1-poly surface micromachined structures with the presented packaging techniques. As shown in figure 4(a), the fabrication started with a 2-poly surface micromachined process. The first poly-silicon (poly0) acted as the conducting/grounding layer and the second poly-silicon (poly1) acted as the structural layer. As illustrated in figure 4(b), the Cr and Cu films were then evaporated and patterned to perform as the electroplating adhesive layer and the seed layer, respectively. It was necessary to properly

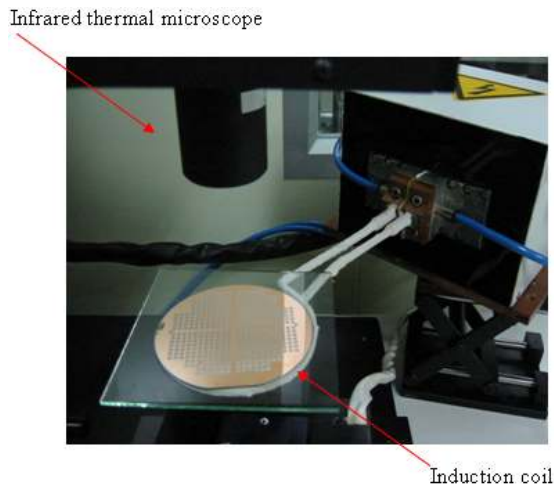


Figure 6. The experiment set-up in this study for induction heating. The sample was placed on top of a magnetic coil. The temperature distribution of the sample was inspected by an infrared microscope.

cover the conducting wire formed by the poly0 layer using the Cr/Cu films. As shown in figure 4(c), a thick photoresist was spun on and patterned using photolithography. The patterned photoresist was exploited as a mold to electroplate the thick Ni/Co alloy spacer. Since the poly0 layer was properly covered by the Cr/Cu films, the step height of the conducting wire could be sealed by the electroplated Ni/Co spacer. After a

$10\ \mu\text{m}$ thick solder was electroplated on top of the Ni/Co alloy, the sacrificial layer was etched away to release the poly-silicon surface structures. As shown in figures 4(d) and (e), the silicon substrate with surface micromachined devices was covered with a glass cap after the localized bonding process. Hence, the poly0 conducting wires acted as feed-through cables.

The SEM photograph in figure 5(a) shows the electroplated Ni/Co spacer on the substrate, and a 4×4 micro-torsional-mirror array inside an $850\ \mu\text{m} \times 550\ \mu\text{m}$ region. The spacer was $50\ \mu\text{m}$ in height, allowing for a large space in the out-of-plane direction for the torsional mirrors. The close-up photograph in figure 5(b) shows the conducting wires and the mirror bonding pads. The conducting wires acted as feed-through cables to connect the pads and the mirrors after encapsulation of the mirror array. In addition, the SEM photograph in figure 5(c) shows the microscopic section of the bonding region. It is found that the $0.5\ \mu\text{m}$ step height poly0 conducting wire was perfectly sealed by the Ni/Co spacer.

3. Testing

According to the basic principles of induction heating, heating efficiency should significantly decay in micro-scale thin film [10]. This study has conducted four different tests, including temperature distribution, bonding strength, leakage and feed-through, to evaluate the performance and feasibility of the bonding process.

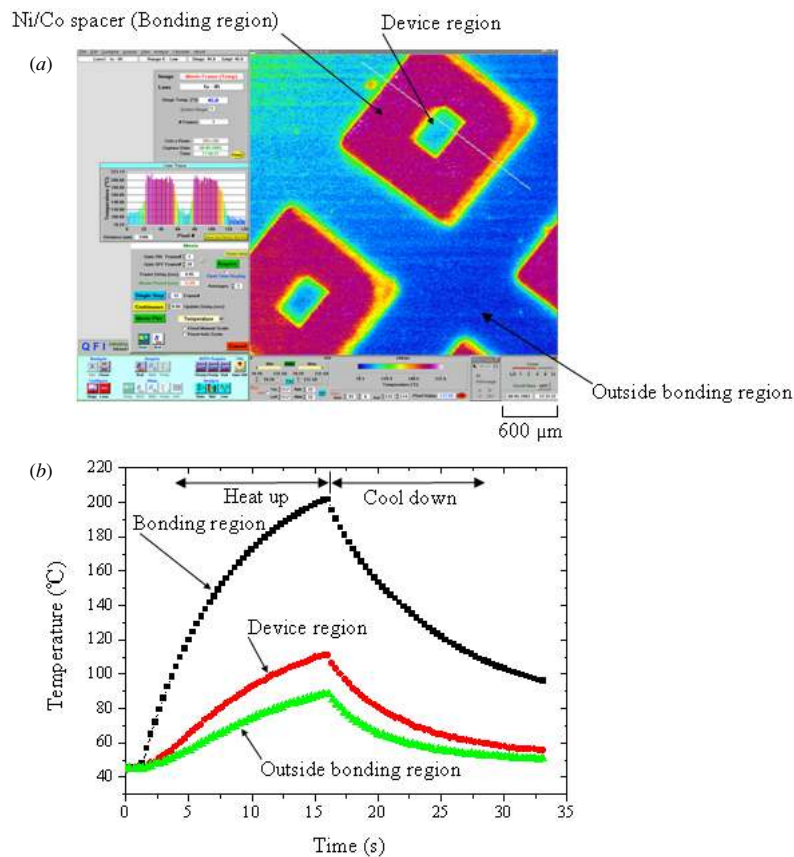


Figure 7. The measured temperature of the test sample during induction heating (a) spatial distribution, and (b) temporal distribution.

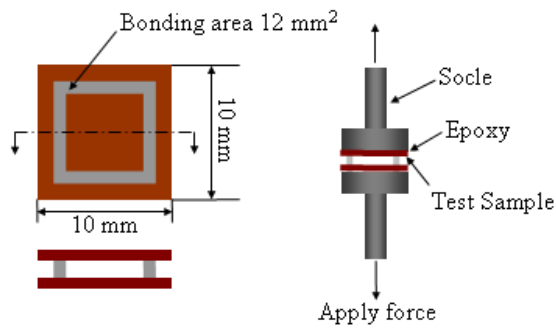


Figure 8. The experiment set-up for evaluation of bond strength. The sample was under a tensile test.

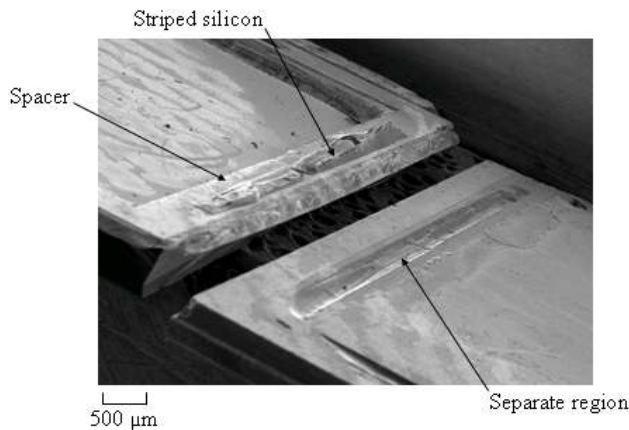


Figure 9. The SEM photograph of the specimen and its bonding region after striped away.

3.1. Temperature distribution

The measurement set-up for the localized heating process is shown in figure 6. Briefly, the substrate was placed on top of the induction coil. Because the whole wafer can be placed inside the magnetic field, the wafer level packaging can be realized. An infrared thermal microscope was used to monitor the temperature distribution during heating. The spatial resolution ranges from $3\ \mu\text{m}$ to $60\ \mu\text{m}$ and the temperature resolution of the infrared thermal microscope is $0.1\ ^\circ\text{C}$. Figure 7(a) shows typical measurement results. The measured temperature distribution of the sample was displayed by colors. The temperature distribution of the specimen during bonding can be characterized as the following three regions: device region, bonding region and outside bonding region. Figure 7(b) shows the quantitative temperature distribution measured from these three regions during the heat-up and cool-down processes. Moreover, figure 7(b) also shows the variation of the specimen temperature with the heating and cooling time. It took 15 s for the bonding region to exceed a temperature of $200\ ^\circ\text{C}$, so as to enable the solder to reflow. Under such a circumstance, the Si-Si or the Si-glass will be bonded by the solder. Since the bonding process was completed within a few seconds, the temperature rise of the device region due to thermal conduction was not significant. Accordingly, the temperature of the device region surrounded by the spacer was only $110\ ^\circ\text{C}$, so that the thin film devices inside this region would not be damaged. In addition, the

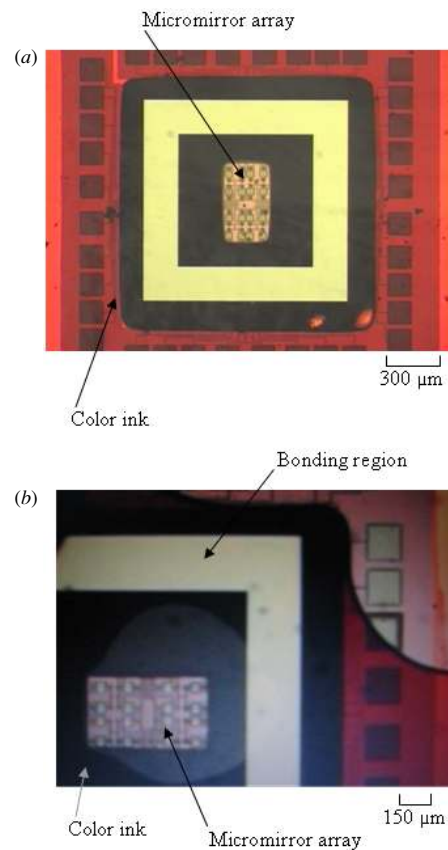


Figure 10. The liquid leakage test for the chip after the 1 h test using color ink.

maximum temperature outside the bonding region was only approximately $90\ ^\circ\text{C}$.

3.2. Bond strength and leakage/feed-through test

The mechanical strength of the bonded specimen was measured using a tensile test. As shown in figure 8, the size of the test sample was $10\ \text{mm} \times 10\ \text{mm}$. The bonded area as indicated in the figure was $12\ \text{mm}^2$. During the test, the sample was fixed between two socles by epoxy and then loaded by a mechanical force, as shown in figure 8. The bonding strength measured for eight different tests ranged from 10.6 MPa to 18.3 MPa. After the tensile test, the broken sample was examined under SEM, as shown in figure 9. It was found that the sample was not separated at the solder bonding region. Moreover, part of the damaged region was at the silicon substrate as indicated in figure 9.

A bonded sample was also immersed in color ink to conduct the leakage test of liquid. Figure 10 shows that no leakage occurred for the 1 h test. The test results show that this bonding approach can be exploited to protect the micromachined structures during the dicing process. The results also indicate that the step height of the conducting wires was perfectly covered by the electroplated Ni/Co alloy. In addition, the rough surface of the electroplated Ni/Co was fully filled with the solder after reflow. A helium leakage test is required to further demonstrate the hermeticity of the packaged device.

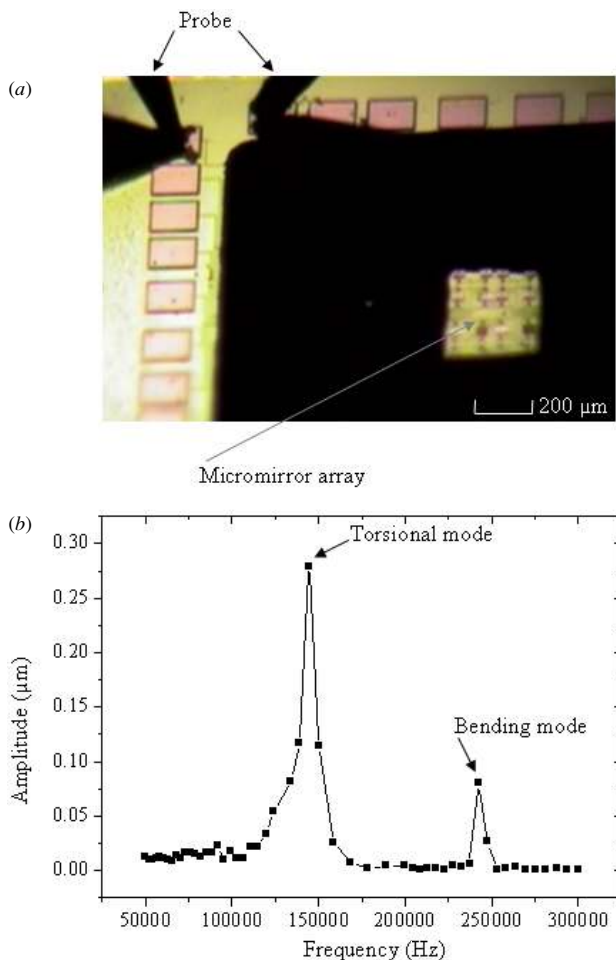


Figure 11. (a) the driving test of the surface micromachined mirror after bonding, and (b) the typical measured frequency response.

Figure 11(a) shows the driving test of the surface micromachined mirror after bonding. The driving ac signal was imported from the bond pad via the feed-through cable to the mirror surrounded by spacer. The typical measured frequency response of the mirror driven by a 150 V voltage is shown in figure 11(b). The test results demonstrate that the feed-through wire successfully transported the driving voltage to the mirror isolated by the bonding ring.

4. Conclusions

The localized induction heating and solder reflow bonding assisted wafer level package has been successfully demonstrated in this study. The experimental results show that it took less than 1 min to complete the bonding process. The MEMS devices experienced a temperature of only 110 °C during bonding, low enough so that the thin film materials would not be damaged. Moreover, the bond strength between silicon and silicon wafer was found to be higher than 18 MPa.

In summary, four advantages are available through this approach. First, the magnetic induction coil will only heat up magnetic materials, such as nickel and cobalt, to a very high temperature within several seconds. Hence, localized heating is realized. Second, the low temperature electroplating process can integrate with various fabrication processes, such as MUMPs and CMOS. Third, the electroplated nickel and cobalt alloy can also perform as a spacer for MEMS devices. Fourth, the step height of the feed-through wire is sealed by the electroplated film, and the flatness and roughness of the electroplated surface are recovered by the solder reflow. Thus, the package for preventing water leakage could be achieved.

Acknowledgments

This project was (partially) supported by the Ministry of Economic Affairs, ROC under no 92-EC-17-A-07-S1-0011 and the Walsin Linwa Corp. The authors would also like to appreciate the NSC Central Regional MEMS Center (Taiwan), the Nano Facility Center of National Tsing Hua University and the NSC National Nano Device Laboratory (NDL) in providing the fabrication facilities.

References

- [1] Fung C D, Cheung P W, Ko W H and Fleming D G (eds) 1985 *Micromachining and Micro Packaging of Transducers* (Amsterdam: Elsevier)
- [2] Kovacs G T A 2000 *Micromachined Transducers Sourcebook* (New York: McGraw-Hill)
- [3] Cheng Y T, Hsu W T, Najafi K, Nguyen T C and Lin L 2002 Vacuum packaging technology using localized aluminum/silicon-to-glass bonding *J. Microelectromech. Syst.* **11** 556–65
- [4] Cao A, Chiao M and Lin L 2002 Selective and localized wafer bonding using induction heating *Technical Digest of Solid-State Sensors and Actuators Workshop (Hilton Head Island, NC, June 2000)* pp 153–6
- [5] Harpster T J and Najafi K 2002 Long-term testing of hermetic anodically bonded glass-silicon packages *MEMS 2002 IEEE Int. Conf. (Las Vegas, NV, 20–24 January)* pp 423–6
- [6] Krassow H, Campabadal F and Tamayo E L 2000 Wafer level packaging of silicon pressure sensors *Sensors Actuators A* **82** 229–33
- [7] Sparks D, Queen G, Weston R, Woodward G, Putty M, Jordan L, Zarabadi S and Jayakar K 2001 Wafer-to-wafer bonding of nonplanarized MEMS surfaces using solder *J. Micromech. Microeng.* **11** 630–4
- [8] Niklaus F, Enoksson P, Kalvesten E and Stemme G 2001 Low-temperature full wafer adhesive bonding *J. Micromech. Microeng.* **11** 100–7
- [9] Reus R D *et al* 1998 Reliability of industrial packaging for microsystems *Microelectron. Reliab.* **38** 1251–60
- [10] Stansel N R 1949 *Induction Heating* (New York: McGraw-Hill)
- [11] Guy A G 1976 *Essentials of Materials Science* (New York: McGraw-Hill)
- [12] Hagemeyer D J 1990 *Fundamentals of Eddy Current Testing* (Columbus, OH: The American Society for Nondestructive Testing, Inc.)